

The Squat of a Vessel with a Transom Stern

Lawrence J. Doctors and Alexander H. Day

The University of New South Wales, Sydney, NSW 2052, Australia

The University of Glasgow, Glasgow, G12 8QQ, Scotland

Summary

The inviscid linearized near-field solution for the flow past a vessel with a transom stern is developed within the framework of classical thin-ship theory. However, the hollow in the water behind the stern is represented here by an extension to the usual centerplane source distribution employed to model the hull itself. As a consequence, the resistance, sinkage, and trim can be computed by means of an integration of the resulting pressure distribution over the wetted surface of the vessel. Comparison of the theoretical results with a systematic series of twelve models shows good correlation with the towing-tank data.

1 Introduction

Previous work on the subject of prediction of resistance of marine vehicles, such as monohulls and catamarans, has shown that the *trends* in the curve of total resistance with respect to speed can be predicted with excellent accuracy, using the traditional Michell (1898) wave-resistance theory.

These principles were advanced in the research of Doctors and Day (1997). There, transom-stern effects were included in the theory by accounting for the hollow in the water behind the vessel in an approximate manner. The wave resistance was assumed to be simply that of the vessel plus its hollow in the water behind the transom. To this drag they added the so-called hydrostatic resistance, which represents the drag associated with the transom stern not being wetted. A good level of correlation between the predictions and the experimental data for a large set of conditions for the tests on a towing-tank catamaran model was demonstrated.

In the current work, we will compute the near-field solution to the flow using the classical thin-ship approximation. This idea clearly represents a considerable addition to the complexity of the solution which contrasts with the traditional far-field method.

2 Mathematical Formulation

Figure 1(a) shows the main geometric features representing a typical hull. The hollow that is developed in the water behind the transom stern is also depicted. A regular meshing, consisting of flat panels or “facets” possessing a rectangular base, is employed for the purpose of the numerical calculation of the pressure, or profile, resistance. This type of panel is algebraically simpler than the “pyramids” or “tents” which were previously employed. The use of flat facets implies a higher level of discontinuity on the hull surface. On the other hand, numerical convergence tests for wave resistance, based on the two types of panels, showed that a similar number of panels was required in either case; namely, 40 panels in the longitudinal direction and 8 panels in the vertical direction.

The solution for the potential due to a point source of strength Q , obtained by Wehausen and Laitone (1960, p. 484, Equation (13.36)), is

$$\phi = -\frac{Q}{4\pi r} + \frac{Q}{4\pi r'} + \varphi, \quad (1)$$

where we have defined

$$r = \sqrt{(x - x')^2 + (y - y')^2 + (z - z')^2}, \quad (2)$$

$$r' = \sqrt{(x - x')^2 + (y - y')^2 + (z + z')^2}, \quad (3)$$

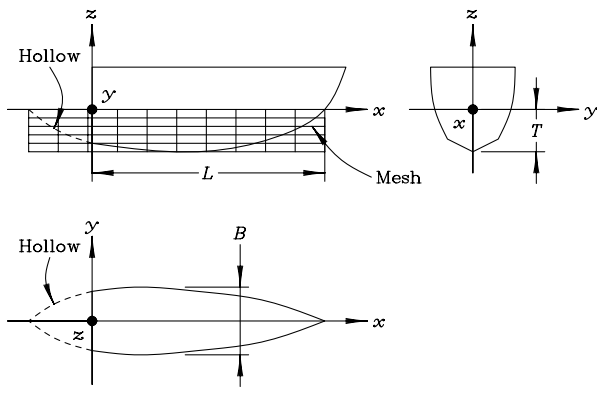


Figure 1: Definition of the Problem
(a) Fitting Mesh to the Vessel

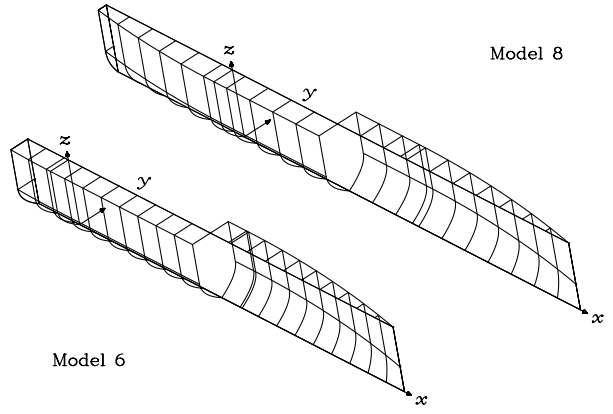


Figure 1: Definition of the Problem
(b) Lego Model 6 and Model 8

and

$$\varphi = -\frac{Qk_0}{4\pi^2} \int_{-\pi}^{\pi} d\theta \int_0^{\infty} dk \frac{\exp\{k[z+z' + i(x-x')\cos\theta + i(y-y')\sin\theta]\}}{k_0 - k\cos^2\theta - i\mu\cos\theta}. \quad (4)$$

The first term in Equation (1) can be integrated for a constant-strength source panel and a constant-slope field panel in the so-called Galerkin manner. The result for the induced longitudinal gradient of the potential at the field panel is

$$\phi_{x,1} = -\frac{1}{4\pi} \sigma_j \sum_{l=-1}^1 w_l \sum_{m=-1}^1 w_m \cdot G_4(i, j, l, m), \quad (5)$$

in which G_4 is the third integral of the $1/r$ function, with respect to z , x , and z , and is just

$$G_4(x, z) = \frac{1}{2} z^2 \sinh^{-1}(x/|z|) + xz \sinh^{-1}(z/|x|) - \frac{1}{2} x \sqrt{x^2 + z^2}. \quad (6)$$

The weighting factor is given by the formula

$$w_l = \begin{cases} -1 & \text{for } l = -1 \\ 2 & \text{for } l = 0 \\ -1 & \text{for } l = 1 \end{cases} \quad (7)$$

and the required arguments in Equation (6) are defined by

$$x = x_i - x_j + l\Delta x, \quad (8)$$

$$z = z_i - z_j + m\Delta z. \quad (9)$$

The third term can also be integrated with respect to the wavenumber k , as well as with respect to the spatial coordinates, to yield

$$\phi_{x,3} = -\frac{i}{2\pi^2 k_0^2} \sigma_j \int_{-\pi/2}^{\pi/2} \cos^3\theta \sum_{l=-1}^1 w_l \sum_{m=-1}^1 w_m \cdot F_4(Z(i, j, l, m)) d\theta. \quad (10)$$

Here, the special complex wave function F_4 is closely related to the exponential integral and was defined by Doctors and Beck (1987). The argument is given by

$$Z(i, j, l, m) = k(z_i + z_j + m\Delta z) + ik_x(x_i - x_j + l\Delta x). \quad (11)$$

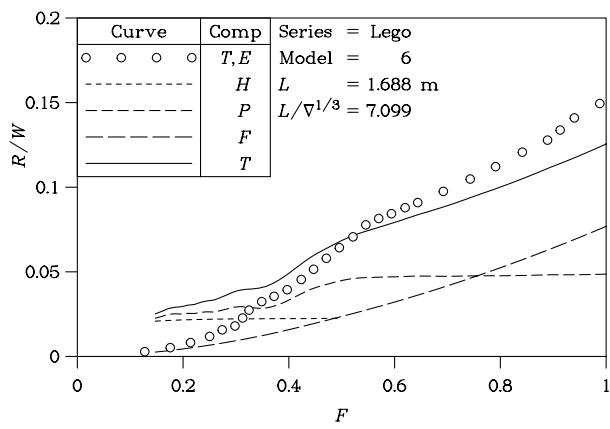


Figure 2: Resistance Components
(a) Lego Model 6

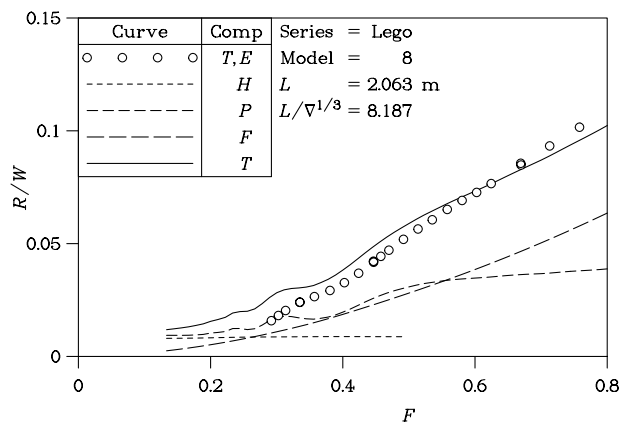


Figure 2: Resistance Components
(b) Lego Model 8

Once the total gradient of the potential at the field panels has been computed, one can determine the pressure on the surface of the hull. The forces and moments on the vessel are then found from this pressure distribution. Initially, the vessel will not be in equilibrium. Numerical experiments showed that using the traditional *hydrostatic stiffness* coefficients worked well for iterating the sinkage and trim of the vessel.

3 Experiments and Numerical Results

The twelve so-called Lego towing-tank ship models were constructed from up to seven segments. The philosophy behind the models is the original Wigley (1934) simple ship. The bow and stern segments have parabolic waterplanes. The bow segments, stern segments, and the parallel middle-body segments all possess parabolic cross sections. Figure 1(b) shows pictorial views of two of the test models. Each model had a beam of 0.150 m and a draft of 0.0938 m. Model 6 had a length of 1.688 m and a prismatic coefficient of 0.8494. Model 8 had a length of 2.063 m and a prismatic coefficient of 0.8275.

Figure 2 shows the resistance components for the two models. The curves show respectively the total-experimental, low-speed hydrostatic, pressure, frictional, and total-theoretical resistance, as functions of the Froude number. The calculations include the effects of sinkage and trim and employ the near-field theory. One sees that the total-theoretical resistance correctly approaches the theoretical hydrostatic resistance at sufficiently low speeds. Of course, the theory ignores real-fluid effects of a partially filled transom hollow; hence the total-theoretical resistance overestimates the total-experimental resistance at low speeds. The correlation could no doubt be improved at higher speeds by employing a form factor to the 1957 International Towing Tank Committee (ITTC) formula for the frictional resistance.

Four theories are compared with experiments on Model 6 in Figure 3(a). In two of the theoretical cases, the model has been free to sink and trim. In two of the theoretical cases, the current near-field approach has been used, while in the other two theoretical cases it is has not (the traditional far-field approach has been used, instead). It is seen that the worst prediction occurs if the experimental sinkage and trim are used in a far-field method, while the current approach apparently gives the second best agreement. Consideration of a form factor would alter the veracity of this statement. Figure 3(b) shows data for Model 8, where one sees that the current theory provides the best correlation.

Finally, we present a comparison for the dimensionless sinkage and the dimensionless trim in Figure 4. Remarkably good agreement is demonstrated for both Model 6 and Model 8.

4 Conclusions

Future research should be directed toward a refinement of the model detailing the precise shape of the transom-stern hollow. Details of the numerical procedure can also be improved, particularly by establishing a data bank of near-field influence functions.

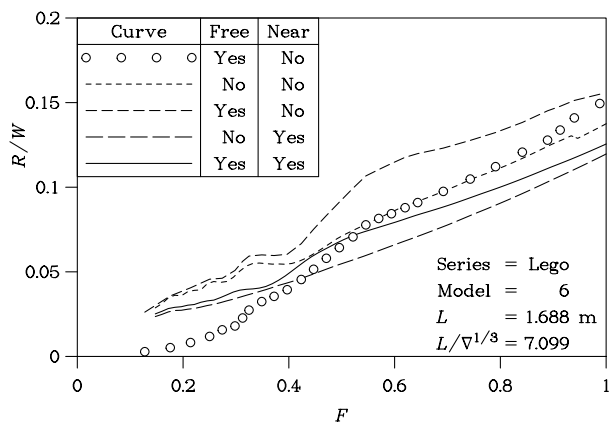


Figure 3: Total Resistance Predictions
(a) Lego Model 6

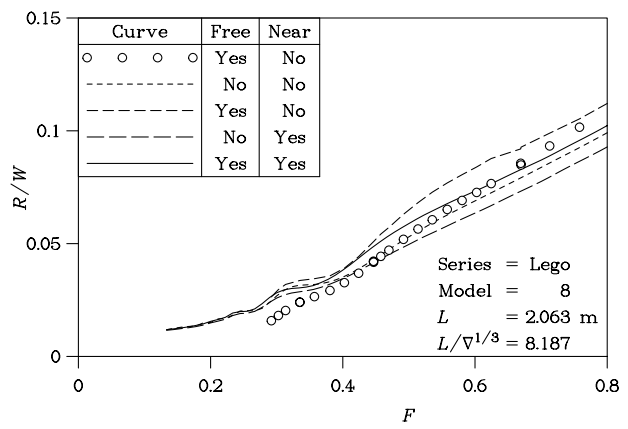


Figure 3: Total Resistance Predictions
(b) Lego Model 8

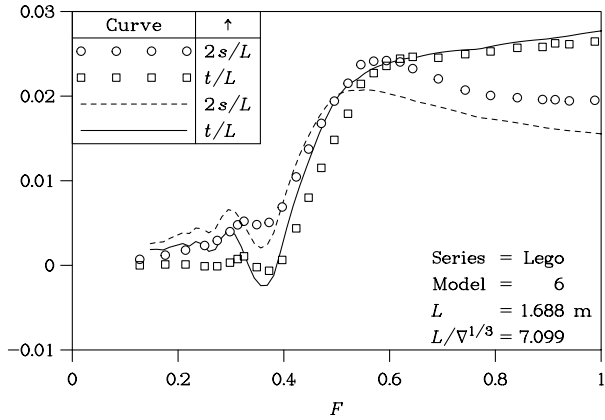


Figure 4: Sinkage and Trim Predictions
(a) Lego Model 6

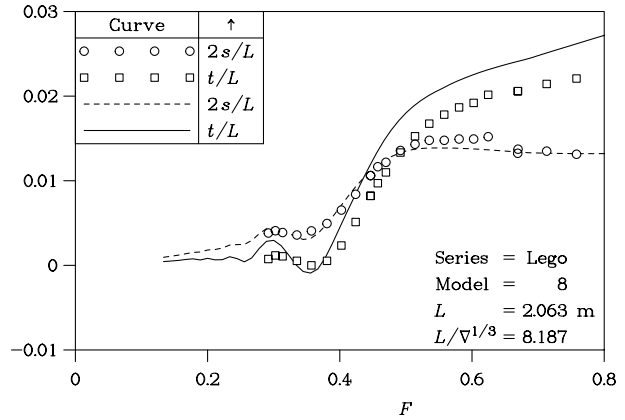


Figure 4: Sinkage and Trim Predictions
(b) Lego Model 8

5 Acknowledgments

The authors would like to thank the Directorate of Naval Platform Systems Engineering, Department of Defence, for its support through Contract 9627MZ. They also gratefully acknowledge the assistance of the Australian Research Council (ARC) Large Grant Scheme (via Grant Number A89917293).

6 References

- DOCTORS, L.J. AND BECK, R.F.: "Convergence Properties of the Neumann-Kelvin Problem for a Submerged Body", *J. Ship Research*, Vol. 31, No. 4, pp 227–234 (December 1987)
- DOCTORS, L.J. AND DAY, A.H.: "Resistance Prediction for Transom-Stern Vessels", *Proc. Fourth International Conference on Fast Sea Transportation (FAST '97)*, Sydney, Australia, Vol. 2, pp 743–750 (July 1997)
- MICHELL, J.H.: "The Wave Resistance of a Ship", *Philosophical Magazine*, London, Series 5, Vol. 45, pp 106–123 (1898)
- WEHAUSEN, J.V. AND LAITONE, E.V.: "Surface Waves", *Encyclopedia of Physics: Fluid Dynamics III*, Ed. by S. Flügge, Springer-Verlag, Berlin, Vol. 9, pp 445–814 (1960)
- WIGLEY, W.C.S.: "A Comparison of Experiment and Calculated Wave-Profiles and Wave-Resistances for a Form Having Parabolic Waterlines", *Proc. Royal Society of London*, Series A, Vol. 144, No. 851, pp 144–159 + 4 plates (March 1934)